Turkish Journal of Electrical Engineering & Computer Sciences

http://journals.tubitak.gov.tr/elektrik/

Research Article

Turk J Elec Eng & Comp Sci
(2022) 30: 1525 – 1538

doi:10.55730/1300-0632.3863

A novel crimping technique approach for high power white good plugs

Ömer Cihan KIVANÇ[1*], Okan ÖZGÖNENEL[2], Ömer BOSTAN[3], Şahin GÜZEL[3], Mert DEMİRSOY[3]

[1]Electrical and Electronics Engineering Department, Faculty of Engineering, İstanbul Okan University, İstanbul, Turkey

[2]Department of Electrical and Electronics Engineering, Samsun Ondokuz Mayıs University, Samsun, Turkey

[3]DEKA Electrotechnic Corporation, Kocaeli, Turkey

Received: 14.09.2021 • **Accepted/Published Online:** 12.04.2022 • **Final Version:** 31.05.2022

Abstract: The crimping process is essential to human health and the durability of devices, especially in domestic appliances. Moreover, terminal crimping is critical to the safe transmission of electricity; incorrect crimping leads to problems including overheating of the plug, power loss, arc, and failure of the mechanical connection. In recent years, analysis has been performed by the finite element method (FEM) to prevent the incorrect design of crimping and to develop higher performance crimping techniques. A novel crimping technique for domestic appliances requiring high-powered plugs is proposed in this study. After defining the crimp parameters and the materials that are used for the crimp design, optimization is undertaken by using an analytical solver that uses both numerical calculation and finite element method analysis by $COMSOL^{TM}$ and Hyperworks. Prototypes are manufactured based on the result of the research, and capability analysis is performed using a histogram diagram. The feasibility and effectiveness of the proposed crimping technique for high-powered applications are validated by simulation and experimental studies.

Key words: Finite element analysis, crimping, histogram diagram, manufacturing technique, capability analysis

1. Introduction

Cables for white goods have become more reliable due to the use of today's technology processes and analysis approaches. The safety of cables has been subjected to special operations by consumer demands, and international standards are crucial both for device safety and human life [1]. Open-ended, soldered, punch down, crimped, and injection techniques are used for white goods cables following industrial standards dependent on the power level of the automotive, domestic appliance, or other device application [2]. At the end of production, products are subject to relevant industrial testing. Testing terminal crimping in white good cables for failure or loose contact is carried out using automatic machines or manual equipment [3].

Crimping is performed by tightening and deforming the open or closed terminal foot on the cable with mechanical pressure, which is a method called cold welding [4]. It is an interface that provides mechanical strength so that the cable cannot be decoupled from the terminal and creates a connection between the cable and the terminal without gas or air permeability [5], [6]. The main challenge in crimping is that mechanical power and electrical efficiency change in inverse proportion. High crimp power increases electrical efficiency in practice while reducing mechanical power [7]. The domestic appliance market produces more than 200 million

*Correspondence: cihan.kivanc@okan.edu.tr

crimped terminals per year. In a mass-market, production of the plug and its components is critical in the economy and safety.

In recent years, the development of finite element method (FEM) analysis software, material technology, and automation systems has allowed the development of various crimping methods [8], [9]. For this reason, there has been an academic and industrial interest in both crimping devices and crimping techniques.

Research in the literature usually focuses on determining the appropriate crimp shape, developing a crimping technique with an analytical approach, improving crimp quality using FEM, and reviewing the effect of material on crimping quality [10], [11]. The study in [12] examined the crimp height, the design approach, and the importance of thermal strain in terms of the crimp. To reduce heating at crimp points, the ideal pressure height is determined by conducting thermal drying, thermal cycle, and direct blowing tests. In [13], crimp simulation studies are performed using Forge software, taking into account material behaviour and mechanical analysis. The study highlighted the large number of crimps being performed, especially in the field of aviation, and emphasized the importance of such a large number of crimps in terms of both reliability and time savings. Two-dimensional (2D) and three-dimensional (3D) FEM analyses conducted in the study provide important information for simulation studies. The study also performed experimental studies of force displacement, 2D profile development, tensile analysis, and mechanical strength. The study of [14] focuses on the analysis of stretching-clamping, which is a general problem of crimping. In particular, it considers the requirements of positioning in crimping steel core aluminium materials, and presents results of ultrasonic tests on thickness variation and the effect of the ratio of steel-aluminium. In [15], the relationship between crimping and the junction capacitance of the cable iron ring and lug points is examined. The study highlights the positive effects of good crimping on change of resistance at junction points - the main reason for the heating experienced at the lug points, especially in medium voltage lines, is the junction resistance being greater than 50 $\mu\,\Omega$. Factors that affect this value are; crimping pressure, the number of crimp notches, notch placement, and the shape of the crimp notches. The study considers each of these factors of crimp design, investigates 28 configurations and finds a deep-notched, hexagonal configuration to give the most effective junction resistance. In [16], a test approach for pre-control and predictive maintenance to prevent the errors and failures of crimping is developed. It seeks a solution to an ideal curve obtained from a trigonometric approach to determine the losses caused by temperature. Temperature and vibration are determined as the main factors for good crimping, and a reliable crimp is needed, especially in corrosion-prone environments.

Studies in the literature generally propose material, end surface, conductor size, crimp depth, and tensile force to improve crimp quality. Errors and failures are caused mainly by excessive, incomplete, extra crimping, mechanical relaxation and crystallization. Mechanical strength is also decreased by vibration around the crimp. The tests defined in international standards have been designed to ensure that these failures are identified in advance.

Crimp analysis is often performed in studies using finite element (FEM) analysis, using software that includes ANSYS, LS-Dyno, Forge, and $COMSOL^{TM}$ [5], [17]. Data capture techniques are also employed that include an ultrasonic, microscopic camera, and thermal imaging [18], [19]. In [8], analysis of the electromagnetic terminal and cable pressure processes is performed by FEM on three different cross-sectional geometries (square, triangular and circular).

Analyses performed by FEM include electrical junction capacitance, hardness, and pull-out. Most study concludes that square geometry gives the best result. At the end of the analyses, it is seen that square geometry has provided the best result. The study in [20] examined the effects of the heat transfer

and deformation that occur in the cold solder process during crimping on various materials using "Scanning Electron Microscopy (SEM)". In [21], the effects of thermal crimping on electrodes of different materials are studied. Tensile strength tests are conducted on steel, molybdenum, wolfram-iron-nickel, tantalum, niobium, titanium-zirconium-molybdenum metals, and alloys. The Levenberg-Marquardt algorithm is used to design a methodology to analyse different electrodes, including shape, material, and cable lug structure.

The study in [22] compares the performance of copper and aluminium cables, especially in the automotive sector. Although aluminium can reduce vehicle weight, copper is significantly superior in terms of conductivity. In addition, copper is almost twice as resistant to mechanical stress due to its bending strength. In addition, the annealing process of aluminium takes longer. Also, aluminium's thermal coefficient and heat resistance make copper more effective in the crimping process. Aluminium also has the disadvantage of poor corrosion resistance. Due to the inconvenience of the connection designs, arc formation and resistance, temperature increase, and mechanical stresses occur at the two connection points due to the permanent deformations experienced at the connection points during the plug-in process. In this study, a novel crimp shape is proposed considering the crimped cross-section area, tensile strength and temperature variation relationships. In [23], it is observed that the proposed crimp shape underperformed in pull out tests in terms of the increase in strength compared to traditional crimp studies. In [24], the tensile strength test results are analyzed for various crimp forms. On the other hand, there is no failure in the same tests for the proposed method. In [25], the high success rates of crimping processes based on machine learning methods are shown. On the other hand, it is observed that the failure rate of the results obtained in the 6-sigma tests performed within the scope of the proposed study is higher than the proposed methods. In the literature [26], these parameters are analysed for various crimp shapes, and the most appropriate design approach is obtained. In the comparative test studies, measurements are performed for various crimp shapes and presented in this study. The superiority of the developed crimp shape over the crimp shapes in the literature has been demonstrated in this study using FEM analysis and experimental tests. The study proposes a novel crimping method and approach shown in Figure 1 for domestic appliances requiring high-powered plugs that minimise the temperature increase, incompatibility with automation, copper crushing, and mechanical deformation. An analytical approach is used for the design, which is validated by simulation studies and considers the dimensions for the crimp. Iterative methods and qualification analyses are analysed for prototype crimping of the proposed design. In Section 2, the primary motivation of the study is declared, and the design approach of the developed crimp structure and the fundamental quantities are presented. In Section 3, simulation studies of the proposed crimp form are performed using $COMSOL^{TM}$ and Hyperworks. In Section 4, experimental studies and results are presented. Moreover, process capability analyses are carried out, and the results are presented in detail. Simulation and experimental studies verify the feasibility and effectiveness of the proposed crimping technique for high-powered applications.

2. Design approach

Crimping ensures good electrical performance by tightening the terminal feet on the cable with sufficient mechanical pressure. The main aim of the crimping is to provide adequate mechanical pressure so that there is good electrical performance and the cable cannot be removed from the terminal when a reasonable pulling force is applied [27]. In particular, there is a relationship between the design of terminals and crimping, and cable size and terminal design affect the efficiency of the crimping operation [28]. For this reason, it is essential to validate the design using techniques such as FEM analysis.

For optimal crimping, mechanical and electrical properties must both be maximized. Crimping made

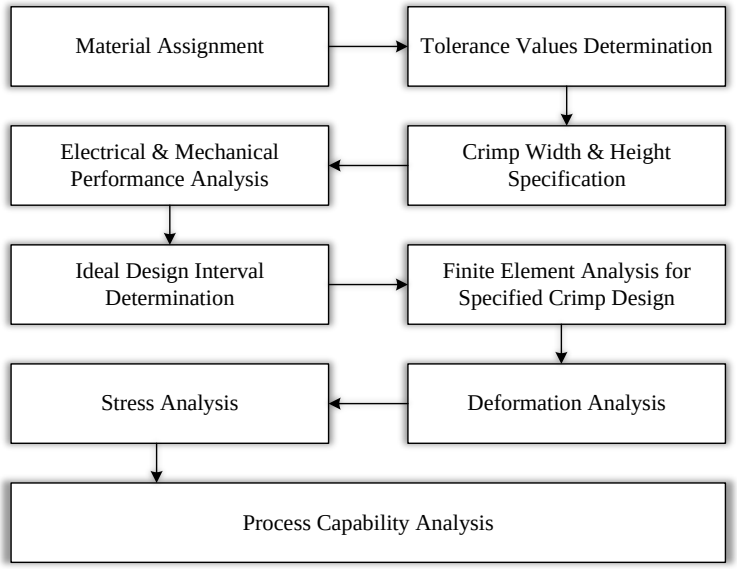

Figure 1. Crimp design approach.

by low pressure does not meet the industrial standards required for electrical conductivity and mechanical deformation and strength. Crimping by high pressure will increase electrical conductivity. However, losses in mechanical properties are experienced, and plastic elongation, copper breakage, and crushing occur due to the plastic deformation in copper wires. Mechanical strength is reduced, especially in the crimping of copper wires with thinner sections. In this case, the thinner copper wires increase the resistance and electrical conductivity is reduced by a further increase in crimp pressure, with an increase in the voltage drop [16]. Figure 2 shows the relationship between mechanical strength and electrical performance as crimp height changes. Crimp design is based on the analysis of mechanical strength and electrical performance as parameters, such as crimp height, are varied to determine the optimal design.

One criterion for the design is to ensure that the isolated feet do not contact the conductive wires by piercing the cable during crimping. This condition can be solved by increasing the height of the crimp. In the experimental study, performance is increased by reducing crimping pressure and using isolated feet that are small compared to the cable cross-section.

Another design criterion is to ensure that the conductive wires become placed so that they are retained firmly. The feet should fully wrap the conducting wires, and the distance to the isolation should be adjusted correctly. The main reasons are to avoid warming to the minimum level for degradation of PVC (Polyvinyl Chloride) and have a mechanical design to ensure that the cable and terminal are parallel. In crimping, the half-rounding must be symmetric, and the terminal conducting feet must support each other. All conductive wires should be designed in a way that there is no air gap between them and are tightened in honeycomb form. A further factor in the design is the ratio of the total crimped area to the noncrimped area. The minimum ratio for the crimp field index, Equation (1), should be 80%, where,

$$S_i = \frac{S_c}{S_{ca} + S_{cl}} x100 \tag{1}$$

S_i refers to the crimping index, S_c refers to the total crimped area, S_{ca}, refers to the non-crimped area caused by the cable, and S_{cl} refers to the noncrimped area caused by the hive. In FEM analysis, crimp efficiency is increased by keeping the "crimp height" to "crimp width" ratio constant. If this ratio differs, then undesirable changes occur to the crimp index. It is also essential to adhere to the crimp force and distance curve, which is shown in Figure 2.

Figure 3 shows the parameters of the crimp design in detail; C_h crimp height, C_w crimp width, C_{mw} measurable crimp width, S_m extrusion height, B_w extrusion width, H_s supporting height, C_d distance between crimp feet, S_b terminal material base thickness, S terminal material thickness, and S_a support angle. The tolerance value for crimp width is generally accepted as ± 0.1 mm. Extrusion height should be the same as the maximum terminal material thickness. The extrusion width should be at most half the terminal material thickness. The bell mouth distance is the distance between the involute bell mouth and the base. This distance should be at least 10% of the terminal material thickness. The difference between the foot bending should be at most half the thickness of the terminal material. The support angle relative to the axis of the foot bend should be less than 30°. The base thickness of the terminal material should be at least 75% of the terminal material thickness.

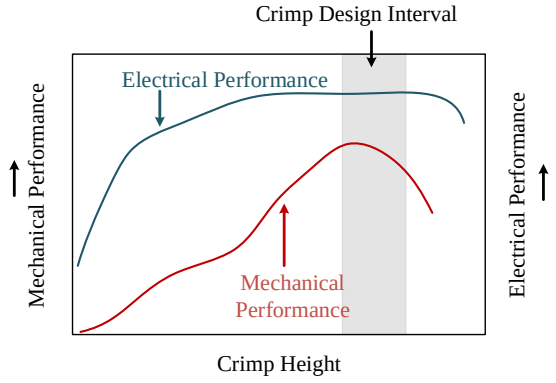

Figure 2. Mechanical and electrical performance and crimp height relationship.

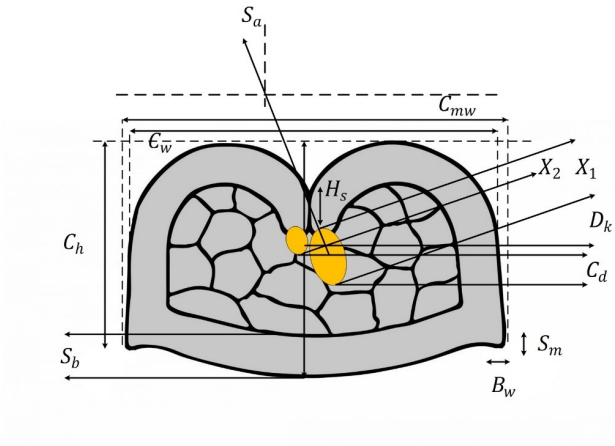

Figure 3. Fundamental dimensions for crimp design.

3. Simulation results

The crimp shape is designed using the approach shown in Figure 4. The crimped structure in Figure 4 is a solid model derived from an image taken using an electron microscope. The preproduction performance of the proposed model has been improved in the simulation using FEM. In order to obtain realistic results, two different physical problems are solved by Equation (2)-(9). The following associated equations are used for electric current and heat transfer physics. In the frequency domain and time-dependent study types of dynamic formulations accounting for both conduction currents and displacement, currents are used [29]. Combining the time-harmonic equation of continuity and generalized to handle current sources yields the following equation,

$$\nabla J = \nabla.(\sigma E + J_e) = -j\omega\rho \tag{2}$$

$$\nabla.D = \rho \tag{3}$$

$$-\nabla.((\sigma + j\omega\epsilon_0).\nabla V - (J_e + j\omega p)) = \theta_j \tag{4}$$

where H is the electric current density, E is the internal energy, ρ is the density, σ is the electrical conductivity, D is the electric displacement, ω is the angular frequency and ϵ_0 is the relative permittivity. For the transient case, using the transient equation of continuity is given in Equation (4) and generalized to handle current sources the resulting equation becomes as in Equation (5) [26], [27], [28].

$$\nabla J = \nabla.(\sigma E + J_e) = -\frac{\partial \rho}{\partial t} \tag{5}$$

$$-\nabla.\frac{\partial(\epsilon_0 \nabla V - p)}{\partial t} - \nabla.(\sigma \nabla V - J_e) = \theta_j \tag{6}$$

The associated equations for heat transfer in solids are given in Equation (6) and Equation (7). The nonisothermal flow in the air is given in Equation (6). The conductive and convective heat transfer inside the air is given in Equation (8) [29], [30], [31].

$$\rho\frac{\partial u}{\partial t} + \rho(u.\nabla u) = -\nabla p + \nabla.\mu(\nabla u + (\nabla u)^T) - \frac{2\mu}{3}(\nabla.u)I \tag{7}$$

$$\rho g\frac{\partial \rho}{\partial t} + \nabla.(pu) = 0 \tag{8}$$

where u is the velocity, μ is the dynamic viscosity and g is the gravity constant [26], [27], [28].

$$\rho C_p\frac{\partial T}{\partial t} + \nabla.(-k\nabla T) = -pC_p u\nabla T + P_{total} \tag{9}$$

where T, P_{total}, and C_p are the temperature, total rated power of crimp region, and specific heat capacity, respectively. The first of these is electrical current (representing the load current) and heat conduction in solids (temperature analysis) methods are used together in Equation (9). The electrical power generated from the current physics is defined as the heat source in the following temperature analysis physics. Conductive thermal analyses are obtained between solid surfaces and solid to air in thermal analyses. The electrical and thermal properties are improved by considering a total of 246 copper conductors and silver-plated folded structures, with the outer area defined as air. Computer simulations are performed under nominal load conditions (32 A and 63 A) and the resulting heat is calculated. Two physical aspects are considered in the simulation; electric current (representing load current) and heat conduction (temperature analysis). The power loss of the crimp region is calculated as 1.93 mW per mm^3. The ambient temperature is set at 20 °C, the simulation time is 60 min to reach stable values and thermal behaviour is observed in the crimp region at one-min intervals. The temperature distribution after 20 min is shown in Figure 5. Figure 6 shows the voltage distribution; 0.15 mV voltage drop is measured on the exterior surface.

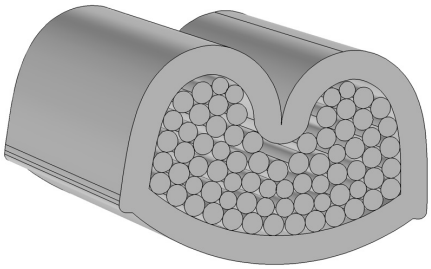

Figure 4. Proposed crimp form.

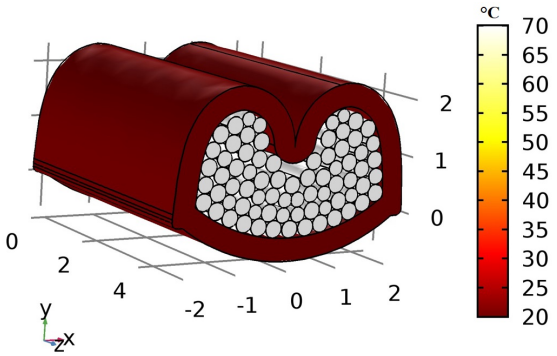

Figure 5. Temperature distribution analysis result.

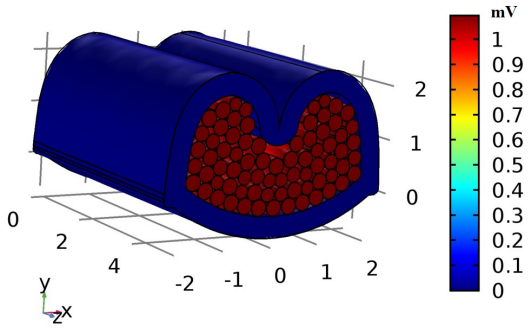

Figure 6. Voltage drop analysis result.

A solid model has been created to analyse the mechanical properties of the proposed crimp design. The model includes the conductive wires, pin ring, pulling tool, jaw to hold the cable, and support section. In the analysis, the support is rigid, the pulling tool applies an axial force on the wires pulling out from the crimp, and the conductors are unconstrained in their movement. The wires are copper, the crimp is phosphor bronze, and the jaw is elastic rigid. The deformation of the jaw is not taken into account and is fixed using rigid elements. The mechanical properties of the copper wires are integrated into the simulation by incorporating the stress-buckling curves obtained from the copper manufacturer. Materials are identified to the simulation using "Johnson-Cook Parameter Identification". The simulation is used to determine the plastic elongation of the copper wires, the force interaction between wires, and the plastic elongation of the phosphor bronze crimp. Critical points have been identified by simulation and validated by practical experiments.

Figure 7 shows the analysis result of plastic elongation formed in the copper wires. Because the plastic elongation values in wires numbered from 1 to 5 are above the breaking elongation, they are determined as wires that fall into the risk group in the analysis. However, they remained at an acceptable value. In other analyses, the results of wires 1-5 are examined and experimental studies are performed for these points, which are considered critical. Figure 8 shows the inter-wire force interaction. In the analysis, all resultant force values are in harmony with neighbouring points and they show incompatibility at only 3 points between a total of 3200 points.

In Figure 9, the plastic elongation on phosphor bronze is presented as a result of the analysis. The reason that the plastic extension on these wires is excessive is that there is too much load on them due to their position. At the end of the simulation, the highest plastic elongation value formed in phosphor bronze material is 15.6% and it is less than the breaking elongation which is at 33%. All wires, except wire 6, are compressed inside the

folds. Based on the simulation, the compressed wires are crushed and there is no air gap. The gap between phosphor bronze and wire is because the coating material is covered by the shell element model. The cross-sectional area of the perpendicular region before compression is measured as 1.69 mm^2. The total area after compression, on the other hand, is 1.26 mm^2. A total contraction of 25.4% is observed in the cross-sectional area. At the end of the simulation studies, it is seen that all wires except the number 6 are compressed by the coating. As a result of the analyses, it is found that the proposed crimping method shows sufficient mechanical, electrical, and thermal performance. Also, the jaw for the experimental studies is designed for the proposed crimp form.

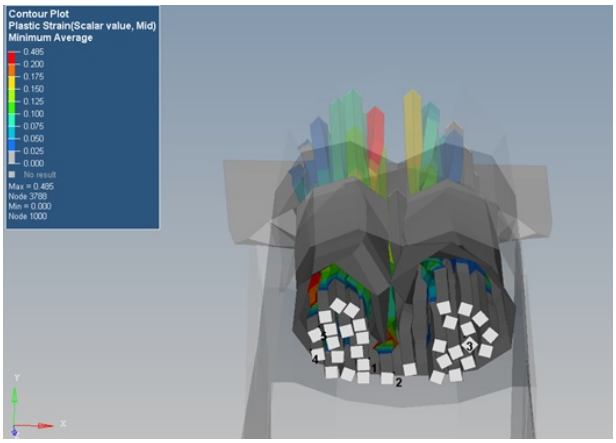

Figure 7. Plastic strain in copper wires.

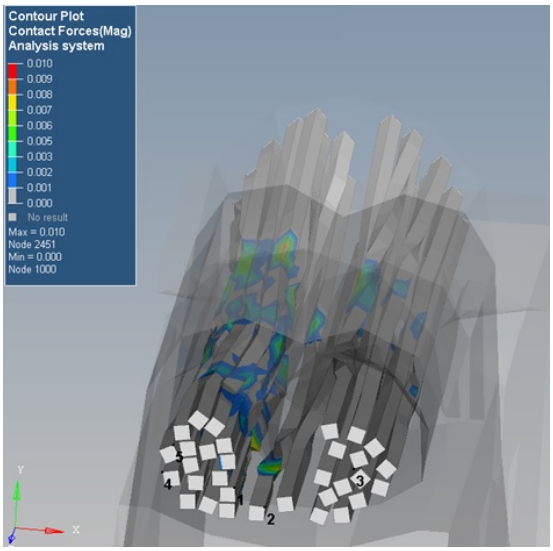

Figure 8. Contact forces between wires.

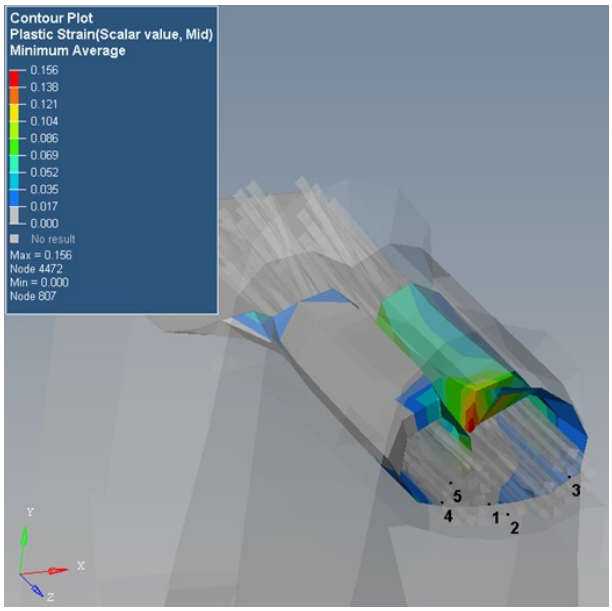

Figure 9. Plastic strain analysis result.

4. Experimental results

The experimental studies have been performed in a test bed with a special design of the jaw shown in Figure 10. The design criteria for the crimping process are validated through the repeated cycle of measuring the characteristic values of the prototypes and refining the FEM model. The aim of the experimental study is to determine the variability in performance arising from elements such as human, material, machine, environment, and method used in the process to create the crimp and ensure the production process is adequate to produce a repeatable performance that remains within tolerance. In this study, the "Histogram Diagram" method is used. In this method, all data must have a normal distribution, and the capability index must be at least 1.67. Calculating control limits according to the capability index, the data is expected to have a normal distribution within these control limits, and if the capability value is greater than or equal to 1.67, this means that the prototype is at the desired capability. However, if these criteria are not met, the process is inadequate, and it is necessary to return to the FEM analysis to refine the design. Capability testing is performed on 125 samples. The data from testing the prototype is used to verify optimal crimp height and tensile breaking force, as in Figure 11.

Figure 10. Experimental test bed.

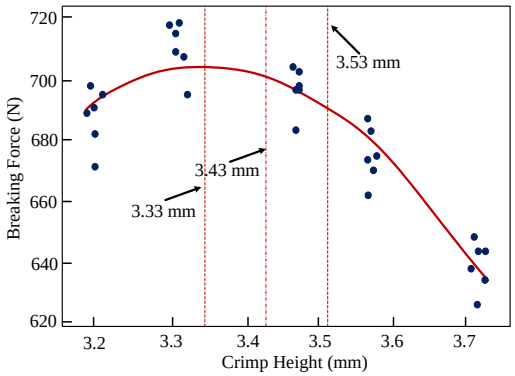

Figure 11. Determination of the ideal range with the relationship between breaking force and crimp height.

Six crimp heights with a difference of 0.08 mm-0.10 mm between heights have been investigated. Six samples are used for each crimp height, and testing is conducted in random order. From the data analysis, the peak of the curve (lower limit point of crimp height) occurs at 3.33 mm. Based on this value, the nominal crimp height value is determined as 3.43 ± 0.05 mm. This reference crimp height is seen as appropriate based on cross-section analysis. A high-resolution cross-sectional area of the prototype corresponding to the optimum crimp height and tensile breaking force is shown in Figure 12. The height of the prototype crimp is measured as 3.434 mm and the crimp area as 4.818 mm^2. Figure 13 and Figure 14 show thermal camera images of temperature distribution at rated currents of 32 A and 63 A in a laboratory environment. Thermal camera images were recorded at 1-min intervals until temperature distribution was stable. The maximum temperature at 32 A load condition was 43.1 °C at the crimp point and 56.2 °C at 63 A. Temperature rise test, mV measurement test, crimp quality measurement, crimp breaking strength are determined according to IEC 62196-1/62196-2 standard. In this study, tests are carried out with reference to the intervals in the standard. Moreover, industrial tests are performed when the pull-out force is equal to or greater than the value required under DIN46249 and IEC 60352-2:2006 standards and is the voltage drop equal to or less than the value prescribed by DIN 46249 and IEC 60352.

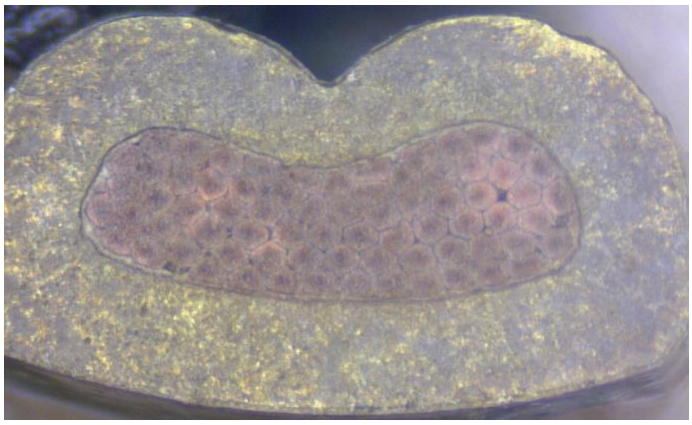

Figure 12. High resolution cross section of proposed crimping method application.

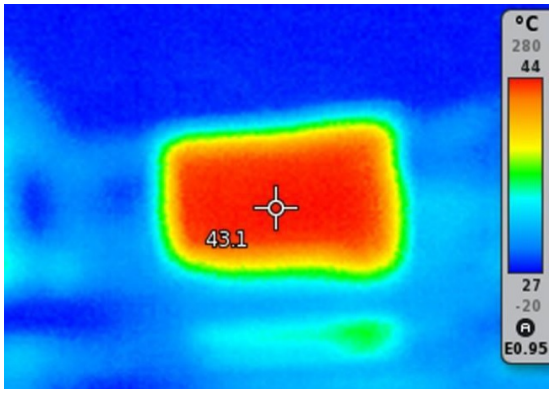

Figure 13. Crimp temperature distribution under 32 A load condition.

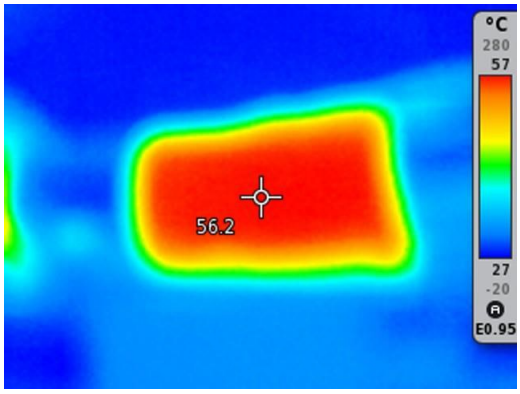

Figure 14. Crimp temperature distribution under 63 A load condition.

The process qualification value for capability analysis was 5.72 for a crimp height of 3.43 ± 0.05 mm, which verifies the process to be sufficient and conforms with the 6σ approach. Capability analysis results are

presented in Figure 15-Figure 20. Braking force X bar chart for crimp height which is illustrated in Figure 15 included LCL (lower control limit), UCL (upper control limit), and $\bar{\bar{X}}$ average. Braking force R bar chart for crimp height which is illustrated in Figure 16 included LCL (lower control limit), UCL (upper control limit), and $\bar{\bar{R}}$ average. In Figure 17, the capability histogram and normal distribution for braking force capability analysis are shown, respectively. Crimp height X bar chart for crimp height which is illustrated in Figure 18 included LCL (lower control limit), UCL (upper control limit), and $\bar{\bar{X}}$ average. Crimp height R bar chart for crimp height which is illustrated in Figure 19 included LCL (lower control limit), UCL (upper control limit), and $\bar{\bar{R}}$ average. In Figure 20, the capability histogram and normal distribution for crimp height capability analysis are shown, respectively. The feasibility and effectiveness of the proposed crimping technique are presented using capability analysis for 6σ approach.

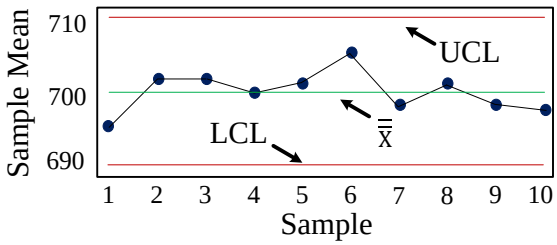

Figure 15. X bar chart for braking force.

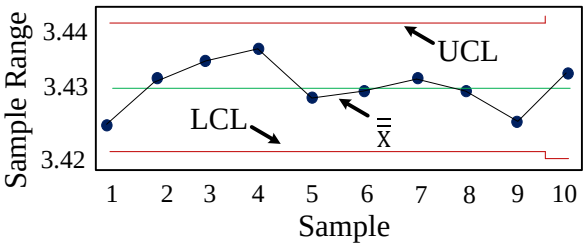

Figure 16. R bar chart for braking force.

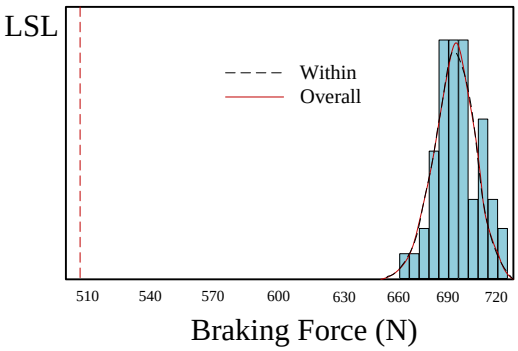

Figure 17. Capability histogram for braking force.

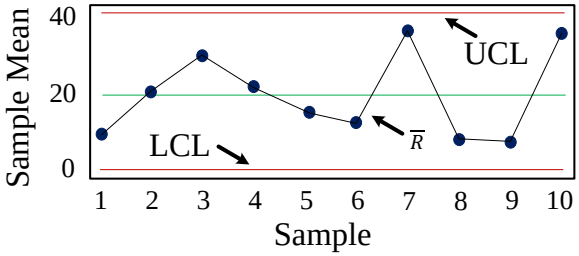

Figure 18. X bar chart for crimp height.

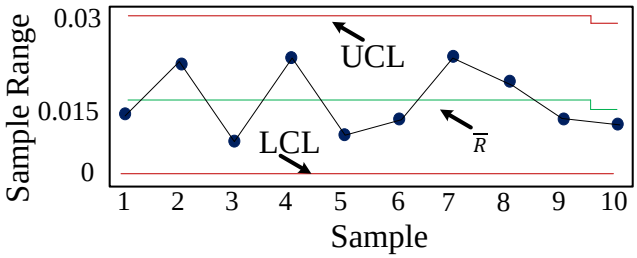

Figure 19. R bar chart for crimp height.

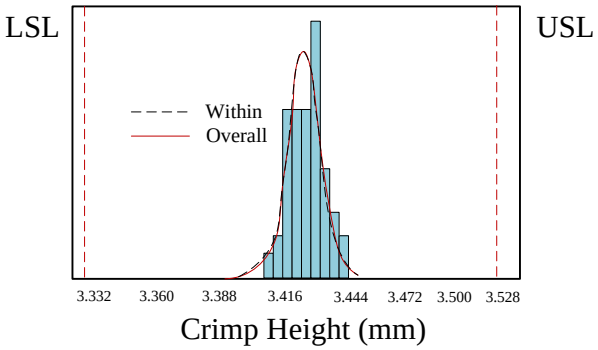

Figure 20. Capability histogram for crimp height.

5. Conclusion

In high-powered domestic appliance applications, crimp quality is essential for human health and to ensure device longevity. Given that more than 200 million plug-in cables are produced each year, it is important to reduce errors and failures resulting from the crimp design and increase the reliability and production capability of companies. A novel crimping method for domestic appliances requiring high-powered plugs is proposed in this study. A novel crimp shape is proposed for white goods, especially considering the arc formation at two connection points due to the permanent deformations experienced at the connection points during the plug-in process due to the inconsistency of the connection designs, and therefore the resistance, temperature increase, and mechanical stress parameters. An analytical approach has been used to design the proposed crimping technique, and all stages of the design have employed FEM analysis. The mechanical, electrical, and thermal performance of the proposed crimping process is analysed in this study. Prototypes have been produced to validate the crimping technique, and test studies are performed. Real-time test studies performed using crimp methods are shown in Figure 21, which are frequently used in literature and industry. Critical parameters are compared in test studies and presented in Table 1. These comparative studies fill an important academic gap in the literature. As a result of the studies, it is observed that the temperature change and breaking force values under the same conditions gave better results with the proposed crimp shape. As a result of the comparisons, 17% less temperature rise and 8% more braking force are obtained using the proposed crimp shape. Adequacy of the prototype is determined from measurements made on a large number of samples and by using an iterative approach to review and redesign the crimping technique.

Crimp shape-1 Crimp shape-2 Crimp shape-3 Proposed crimp shape

Figure 21. Comparison of various crimp shapes.

Table . Experimental results for various crimp shapes.

No	Current	Ambient temp.	Max. temp.	Temp. variation	Breaking force
Crimp-1	32 A	20.8 K	68.4 K	47.6 K ($\triangle$T)	554 N
Crimp-2	32 A	22.1 K	72.4 K	50.3 K ($\triangle$T)	678 N
Crimp-3	32 A	21.4 K	80.4 K	59 K ($\triangle$T)	492 N
Proposed crimp shape	32 A	20.5 K	60.2 K	39.7 K ($\triangle$T)	725 N

Acknowledgment

This work was supported by The Scientific and Technological Research Council of Turkey (TÜBİTAK) (grant 3180026). O.O. and O.B. gave the idea, O.C.K, S.G., and M.D. did the experiments, O.C.K., O.O., and O.B. interpreted the results, O.C.K, O.O., and O.B. wrote the paper.

References

[1] Ocoleanu C, Popa I, Dolan A, Ivanov V. Crimped connections heat transfer coefficient law determination using experimental and numerical results. In: International Conference on Applied and Theoretical Electricity; Craiova, Romania; 2014. pp. 1–4.

[2] Beloufa A. The effect of cable section on the variation of power automotive connector temperature. IEEE Transactions on Components, Packaging and Manufacturing Technology 2019; 9 (6): 1020-1028. doi: 10.1109/TCPMT.2019.2914894

[3] Shirgaokar M. Optimization of mechanical crimping to assemble tubular components. Journal of Materials Processing Technology 2004; 146: 35–43. doi: 10.1016/S0924-0136(03)00842-2

[4] Villeneuve K, Petitprez M, Bouchard PO, Desjean C. Dynamic finite element analysis simulation of the terminal crimping process. In: 8th International Conference on Electrical Contact; Chicago, USA; 1996. pp. 156–172.

[5] Özgönenel O, Bostan O, Guzel S. 2D simulation of crimping process for electric vehicle battery charge cable. In: COMSOL Conference; Lausanne, Switzerland; 2018. pp. 1–7.

[6] Frank RF, Morton CP. Comparative corrosion and current burst testing of copper and aluminum electrical power connectors. IEEE Transactions on Industry Applications 2007; 43 (2): 462–468. doi: 10.1109/TIA.2006.889973

[7] Kivanc OC, Ozgonenel O, Bostan O. New generation plug-in cable design and product development for white goods-cold plug. In: 11th International Conference on Electrical and Electronics Engineering; Bursa, Turkey; 2019. pp. 39–43.

[8] Rajak AK, Kore SC. Comparison of different types of coil in electromagnetic terminal-wire crimping process: numerical and experimental analysis. Journal of Manufacturing Processes 2018; 34 (A): 329–338. doi: 10.1016/j.jmapro.2018.06.025

[9] Mobasher B, Kingsbury D, Montesinos J, Gorur RS. Mechanical aspects of crimped glass reinforced plastic (GRP) rods. IEEE Transactions on Power Delivery 2003; 18 (3): 852–858. doi: 10.1109/TPWRD.2003.813871

[10] Rajak AK, Kore SC. Experimental investigation of aluminium–copper wire crimping with electromagnetic process: its advantages over conventional process. Journal of Manufacturing Processes 2017; 26: 57–66. doi: 10.1016/j.jmapro.2017.01.009

[11] Rajak AK, Kore SC. Numerical simulation and experimental study on electromagnetic crimping of aluminium terminal to copper wire strands. Electrical Power Systems Research 2018; 163: 744–753. doi: 10.1016/j.epsr.2017.08.014

[12] Williams DM, Range ME, Pascucci VC, Savrock JT. Forensic analysis of thermally stressed crimp connections. In: 61st Holm Conference on Electrical Contacts; San Diego, USA; 2015: 331–337.

[13] Mocellin K, Petitprez M, Bouchard PO, Desjean C. Computational modeling of electrical contact crimping and mechanical strength analysis. In: 56th IEEE Holm Conference on Electrical Contact; Charleston, USA; 2010: 1–3.

[14] Xie Y, Wang S, Zhang C, Ouyang K, Jiang X. Study on nondestructive testing methods for crimping quality of steel cored aluminum strand. In: International Conference on Measuring Technology and Mechatronics Automation; Changsha, China; 2018: 78–80.

[15] Ruzlin MMM, Shafi AGH, Basri AGA. Study of cable crimping factors affecting contact resistance of medium voltage cable ferrule and plug. In: International Conference and Exhibition on Electricity Distribution; Stockholm, Sweden; 2013: 1–4.

[16] Ocoleanu CF, Cividjian G, Manolea G. Solutions for quality pre-control of crimp contacts used in electric power systems and electrical machines. In: International Symposium on Environmental Friendly Energies and Applications; Paris, France 2014:1–6.

[17] Katia M, Petitprez M. Experimental and numerical analysis of electrical contact crimping to predict mechanical strength. Procedia Engineering 2014; 81: 2018–2023. doi: 10.1016/j.proeng.2014.10.274

[18] Seefried J, Glabel T, Zurn M, Franke J. Evaluation of monitoring approaches for the ultrasonic crimping process of tubular cable plugs. In: 7th International Electric Drives Production Conference; Wuerzburg, Germany; 2017: 1–6.

[19] Weigelt M, Mayr A, Seefried J, Heisler P, Franke J. Conceptual design of an intelligent ultrasonic crimping process using machine learning algorithms. Procedia Manufacturing 2018; 17: 78–85. doi: 10.1016/j.promfg.2018.10.015

[20] Mroczkowski RS, Geckle RJ. Concerning "cold welding" in crimped connections. In: Forty-First IEEE Holm Conference on Electrical Contacts; Montreal, Canada 1995: 154–164.

[21] Spreng S, Glaessel T, Muselmann J, Worrlein M. Quantification of the influence of varying electrode shapes and materials on the thermo-crimping process of standardized tubular cable plugs. In: 6th International Electric Drives Production Conference; Nuremberg, Germany; 2016: 48–51.

[22] Piyush K, Gautam A, Dayal H, Bora A, Patro CN et al. Selection criteria for usage of aluminum wires in automobile wiring harness. In: IEEE International Transportation Electrification Conference; Chennai, India 2015:1–5.

[23] Saxena R, Sharma SK. Investigation of pulse power technology for crimping of electrical cables. In: IEEE 2nd International Conference on Applied Electromagnetics, Signal Processing, and Communication; Bhubaneswar, India; 2021: 1–5.

[24] Chen Y, Zhang M, Cao R, Xiang Y, Zhang B et al. Reliability study on crimping joint of copper-clad aluminum wire cable in spacecraft. In: 21st International Conference on Electronic Packaging Technology; Guangzhou, China; 2020: 1–5.

[25] Meiners M, Mayr A, Kuhn M, Raab B, Franke J. Towards an inline quality monitoring for crimping processes utilizing machine learning techniques. In: 10th International Electric Drives Production Conference; Ludwigsburg, Germany; 2020: 1–6.

[26] Li P, Liu G, Fan J, Sun J, Xiu H et al. Mathematical model for the tensile strength of the crimping assembly of aviation wiring harness end. Nature Scientific Reports 2021; 11: 1–11. doi: 10.1038/s41598-021-97498-8

[27] Weddeling C, Demir OK, Haupt P, Tekkaya AE. Analytical methodology for the process design of electromagnetic crimping. Journal of Materials Processing Technology 2015; 222: 163–180. doi: 10.1016/j.jmatprotec.2015.02.042

[28] Xiao X, Wang J, Tong Y, Chen L, Cai L et al. Residual mechanical strength evaluation of crimping assembled composite insulators with service time of 10–14 years. IET Generation, Transmission and Distribution 2019; 13 (19): 4324–4330. doi: 10.1049/iet-gtd.2018.5344

[29] Özgönenel O, Thomas D. Modeling and simulation of 2.5 MVA SF6-gas–insulated transformer. Turkish Journal of Electrical Engineering and Computer Sciences 2017; 25: 3475–3485. doi: 10.3906/elk-1708-28

[30] Özgönenel O, Thomas D. SF6 gas-insulated 50-kVA distribution transformer design. Turkish Journal of Electrical Engineering and Computer Sciences 2018; 26: 2140–2150. doi: 10.3906/elk-1708-28

[31] COMSOL. Heat Transfer Module, Version 3.5. Helsinki, Finland: COMSOL, 2008.